sions in the kilovolt range[1], this signifies that electron motions produced by the external field occupy only a very small fraction of the available phase space. Therefore, we can conclude that the electronic motions causing the observed multiphoton excitation possess a very signficant level of order and are not appreciably perturbed by a thermal component[13–15]. □

Received 14 February; accepted 11 July 1994.

1. McPherson, A., Luk, T. S., Thompson, B. D., Boyer, K. & Rhodes, C. K. *Appl. Phys.* B**57,** 337–347 (1993).
2. McPherson, A. *et al. Phys. Rev. Lett.* **72,** 1810–1813 (1994).
3. Borisov, A. B. *et al. Phys. Rev. Lett.* **68,** 2309–2312 (1992).
4. Solem, J. C. & Baldwin, G. C. *Science* **218,** 229–235 (1982).
5. Bouma, B., Luk, T. S., & Rhodes, C. K. *J. opt. Soc. Am.* B**10,** 1180–1184 (1993).
6. Schneider, D. *et al. Phys. Rev.* A**42,** 3889–3895 (1990).
7. Clark, M. W. *et al. Phys. Rev.* A**47,** 3983–3997 (1993).
8. Mazing, M. A. & Shevel'ko, A. P. *Proceedings of the Lebedev Physical Institute* Vol. 179 (ed. Sobel'man, I. I.) 1–50 (Nova Science, Commack, New York, 1988).
9. Contunie, Y, Yaakobi, B., Feldman, U., Daschek, G. A. & Cowan, R. D. *J. opt. Soc. Am.* **71,** 1309–1314 (1981).
10. Keane, C. J., Hammel, B. A., Osterheld, A. L. & Kania, D. R. *Phys. Rev. Lett.* **72,** 3029–3032 (1994).
11. Carlson, T. A., Nestor, C. W. Jr, Wasserman, N. & McDowell, J. D. *Atomic Data* **2,** 63–99 (1970).
12. Augst, S., Strickland, D., Meyerhofer, D. D., Chin, S. L. & Eberly, J. A. *Phys. Rev. Lett.* **63,** 2212–2215 (1989).
13. Boyer, K., Thompson, B. D., McPherson, A. & Rhodes, C. K. *J. Phys.* B (in the press).
14. Thompson, B. D., McPherson, A., Boyer, K. & Rhodes, C. K. *J. Phys.* B (in the press).
15. Boyer, K. & Rhodes, C. K. *J. Phys. B* (in the press).

ACKNOWLEDGEMENTS. The authors thank J. Wright and P. Noel for technical assistance, and S. Guggenheim for the use of his microdensitometer, and A. P. Shevel'ko for measurements with the von Hámos spectrometer. C.K.R. acknowledges discussions with D. Schneider and J. W. Longworth. This work was supported by the US DoE, AFOSR, ONR, SDI/NRL and ARO.

Reduction of frictional forces between solid surfaces bearing polymer brushes

Jacob Klein*, Eugenia Kumacheva*, Diana Mahalu*, Dvora Perahia* & Lewis J. Fetters†

* Department of Materials and Interfaces, Weizmann Institute of Science, Rehovot 76100, Israel
† Exxon Research and Engineering Company, Annadale, New Jersey 08801, USA

THE use of lubricants to reduce friction and wear between rubbing surfaces has been documented since antiquity[1–3]. Recent approaches have focused on boundary lubrication by surfactant-like species coating the surfaces, whereby the friction between them is replaced by the weaker forces required for shear of adhesive contacts between the surfactant layers[3,4]. An alternative approach is to tether polymer chains to the surfaces by one end which, when swollen by a solvent, then act as molecular 'brushes' that may facilitate sliding. The normal forces between sliding brush-bearing surfaces have been previously investigated[5,6], but the lateral forces, which are the most important from the point of view of lubrication, are harder to measure. Here we report the measurement of lateral forces in such a system. We find a striking reduction in the effective friction coefficients μ_b between the surfaces to below our detection limit ($\mu_b < 0.001$), for contact pressures of around 1 MPa and sliding velocities from zero to 450 nm s^{-1}. We believe that this effect is due to the long-ranged repulsion, of entropic origin, between the brushes, which acts to keep the surfaces apart while maintaining a relatively fluid layer at the interface between them.

Normal and lateral forces, $F_{normal}(D)$ and $F_{shear}(D)$ respectively, between curved, molecularly smooth mica surfaces immersed in toluene were determined as a function of the surface separation D and the sliding velocity v_s. The apparatus used, described in detail earlier[5,6], is capable of measuring the forces directly and simultaneously by monitoring the bending of two sets of springs as the surfaces move with respect to each other (Fig. 1, upper inset).

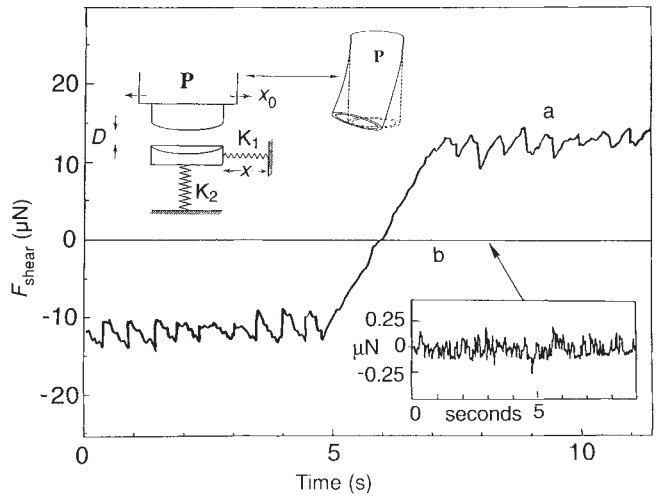

FIG. 1 The variation with time of the shear force F_{shear} between two mica sheets a distance D apart, compressed by a normal load $F_{normal} = 19 \pm 2$ μN, in response to an applied shear. The upper inset shows schematically the configuration of the surfaces mounted on crossed cylindrical lenses. The bending δx and δD of the two orthogonal springs K_1 and K_2 yields the respective forces F_{shear} and F_{normal} (ref. 5). Lateral motion δx_0 is applied to the top surface via the sectored piezocrystal P, whose bending configuration is indicated. The sliding velocities used in the present study were in the range $v_s \equiv d(x_0 - x)/dt = 15$–$450$ nm s^{-1}. Curve **a**, sliding of bare mica surfaces in toluene. $D = 14 \pm 3$ Å, corresponding to two monolayers of toluene between the surfaces. A clear stick–slip behaviour is observed during sliding. The region where the surfaces stick and the shear force changes sign at $t = 5$–7 s indicates a reversal of the sliding direction. The sliding velocity $v_s = 45$ nm^{-1}. Curve **b**, Sliding of mica surfaces covered by a PS−X(1.4×10^5) brush, at $D = 37$ nm. (In this and subsequent data the brushes form from a solution of polymer concentration (6×10^{-5})–(10^{-4}) g ml^{-1}. On the scale of the main figure the shear forces are within the thickness of the line labelled b. The lower inset shows F_{shear} on an expanded scale: the shear force is less than the noise-limited resolution δF_{shear}. There is no measurable change on reversing the sliding direction. The sliding velocity $v_s = 15$ nm s^{-1}

When the mica sheets are compressed in the pure solvent the toluene is squeezed out, until the normal force is balanced by the structural forces due to the final monolayers of solvent remaining between the surfaces, as observed for other liquids[7]. On applying a shear force that exceeds the frictional force, the surfaces slide and their motion displays a characteristic stick–slip behaviour[1], as seen clearly in Fig. 1, curve *a*. Such stick–slip motion has been observed also for mica sheets in other simple liquids[8]. It is in accord with the model of interfacial sliding due to Tabor[4], where the friction F arises from the forces required to shear the adhesive junctions: $F = S_c A$; here S_c is a

TABLE 1 Molecular characteristics of polymers and corresponding brushes

Sample	M_r	M_r/M_n	$2L_M$(nm)	s_M(nm)
PS−X(2.6×10^4)	2.65×10^4	1.02	45	4.6
PS−X(1.4×10^5)	1.41×10^5	1.03	125	9.4
PS−X(3.75×10^5)	3.75×10^5	1.03	230	14.4

Samples were synthesised and characterized as described in ref. 9. The end-group −X is $-(CH_2)_3N^+(CH_3)_2(CH_2)_3SO_3^-$. M_r is the relative weight-averaged molecular mass of the polymer, M_n is its relative number-averaged molecular mass and L_M and s_m are the brush heights and mean inter-anchor spacings determined from the respective $F_{normal}(D)$ profiles (the surface number densities of chains for each brush are given by $(1/s_M)^2$).

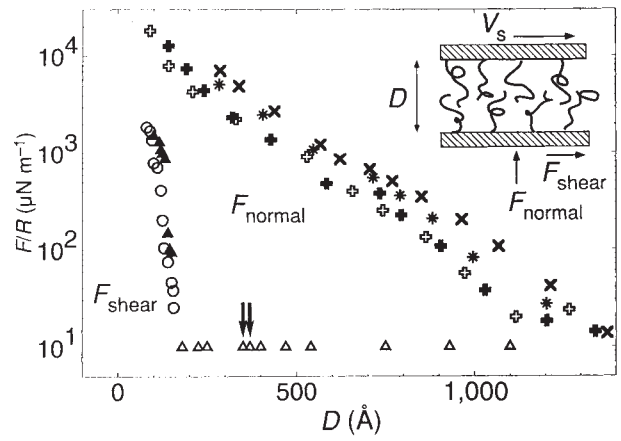

FIG. 2 Normal and shear force profiles, $F_{normal}(D)$ and $F_{shear}(D)$ respectively, between mica surfaces bearing PS−X(1.4×10^5) brushes, as indicated in the diagram. The force axis is normalized with respect to the radii of curvature R (~1 cm) of the mica sheets, which converts $F_{normal}(D)$ to the interaction energy in the Derjaguin approximation (for comparison F_{shear} is similarly normalized). Results from several different experiments are shown. Shear velocities for the $F_{shear}(D)$ measurements were in the range v_s = 15–450 nm s^{-1}. The open triangles (△) at $D>180$ Å correspond to shear forces that are within the noise-limited resolution δF_{shear} of the signal (see Fig. 1, lower inset): as an upper estimate they are all set to equal $|\delta F_{shear}|$. Highlighted F_{shear} data at D = 374 Å and 352 Å (indicated by arrows) were taken at v_s = 15 nm s^{-1} and 450 nm s^{-1} respectively.

critical shear stress which depends on the details of the interfacial region, and A is the contact area.

Following measurements in pure toluene, end-functionalized polystyrene (PS) chains of relative molecular mass M_r, designated PS−X(M_r), where the end-group −X denotes a zwitterion, are added to the solvent. Their characteristics are given in Table 1. The molecules attach spontaneously by their zwitterion-terminated end to the mica surfaces, with the PS chain dangling into the solution[9], to form extended brush-like layers whose structure and normal interactions have been extensively studied[9–12]. Figure 1 curve *b* shows the shear forces required to slide surfaces covered by a PS-X(1.4×10^5) brush at the same normal load as for the pure toluene case. These are some orders of magnitude lower than the forces needed for sliding the bare surfaces, and indeed are within the vibration-limited resolution $\delta F_{shear} \approx \pm 0.1$ μN of the measurement (Fig. 1, lower inset).

The $F_{normal}(D)$ and $F_{shear}(D)$ profiles between the brush-bearing surfaces are shown in Fig. 2 for PS−X(1.4×10^5) over the entire range $D<2L$ of interactions (where $L\approx65$ nm is the thickness of each brush). $F_{normal}(D)$ is repulsive due to osmotic interactions; it increases monotonically at $D<2L$, and is similar to earlier studies[9]. The corresponding shear forces required to induce and maintain interfacial sliding are extremely low. $F_{shear}(D)$ is within the instrumental resolution δF_{shear} down to $D=D_0\approx20$ nm; that is, under normal loads up to $F_{normal}(D=D_0)\approx100$ μN. Defining an effective friction coefficient between the sliding brush-covered surfaces as $\mu_b=(F_{shear}(D)/F_{normal}(D))$, we find $\mu_b<0.001$ (that is, it is smaller than our measurable limit) at these loads. In this regime the behaviour is reversible with respect to surface separation, indicating stability of the brushes to shear. For the regime $2L<D<D_0$, the frictional forces remain immeasurably small for all velocities in the range v_s = 15–450 nm s^{-1}; no frictional force was detectable when the surfaces started moving from rest. Clearly, whatever frictional force remains will be the result of viscous dissipation, and thus velocity dependent—but as it is below our instrumental resolution we cannot quantify this dependence. At higher compressions a stick–slip behaviour similar to that seen in the absence of polymer is observed (Fig. 3 inset), with a measurable $F_{shear}(D)$ which increases rapidly at $D<D_0$ (at the highest compressions there was some indication that the surface-attached polymer was sheared off as the surfaces slid past each other, but following a short period of separation in the PS−X solution, the brushes 'healed' to their original form).

Similar profiles were measured between mica surfaces covered by PS−X(M_r) brushes with $M_r=2.6\times10^4$ and 3.8×10^5. This range of M_r corresponds to a fivefold variation in brush-thickness and tenfold variation in tethered chain density (Table 1). The data is shown in Fig. 3. In this reduced representation, a similar general behaviour is seen for all three brushes: extremely low friction (within the resolution δF_{shear} of the measurements) from $D=2L$ down to a surface separation D_0, and a rapidly increasing frictional force at higher compressions ($D<D_0$). We find that the onset for rapid increase in the friction is at a compression ratio $(D_0/2L)\approx0.1$–0.15 for all three brushes. The ratios of shear to normal forces at $D=D_0$ yield the effective friction coefficients μ_b at these separations, and show that $\mu_b<0.001$ in this regime for all three cases. The corresponding contact pressures P at the points of closest approach is given by ref. 9 as $P=(1/2\pi R)(\partial F_{normal}/\partial D)|_{D=D_0}$. This yields values $P(D_0)\approx(1$–$2)\times10^6$ N m^{-2}, with the higher values for the shorter brushes.

The reduction in the frictional forces afforded by the layers of end-attached polymer chains is of entropic origin. Excluded-volume effects, which reduce the configurational entropy of the chains, dominate the interactions and lead to strong net segmental repulsions in the good-solvent medium[13,14]. The result is a long-range equilibrium separation of the surfaces[9–11]. At the same time theoretical studies suggest only a limited mutual interpenetration of the brushes[15,16], even under compression. This in turn ensures rapid relaxation of the interpenetrating chains as the surfaces slide past each other, and thus a relatively fluid region at the brush–brush interface: hence the low friction. The shear force F_{shear} required to maintain sliding of the brushes arises from the viscous dissipation in the interfacial region asso-

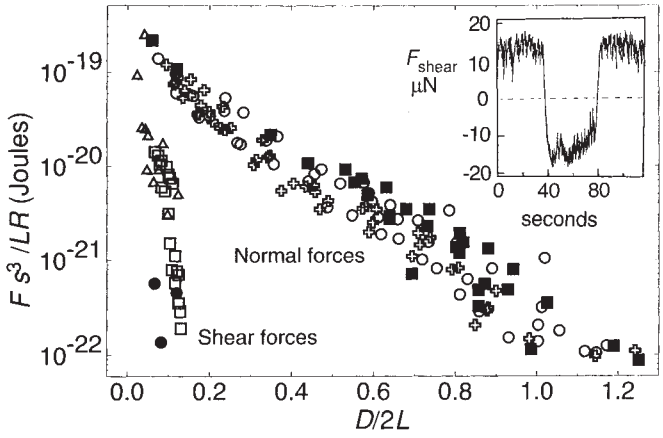

FIG. 3 Normal and shear force profiles for interactions between mica surfaces bearing PS−X(M_r) brushes, plotted as (Fs^3/LR) versus $D/2L$, where $s=s_M$ is the mean spacing between chain anchoring points for the respective brushes, and $L=L_M$ are the respective brush heights. In the Alexander–de Gennes model[10,11] this reduction makes the F_{normal} data independent of M_r. The $F_{shear}(D)$ profiles have been similarly scaled for purposes of comparison. ■, ●, $M_r=2.6\times10^4$; □, ○, $M_r=1.4\times10^5$; △, ◆, $M_r=3.75\times10^5$. Results are shown from two or three experiments for each molecular weight; shear forces smaller than the resolution δF_{shear} are not shown. The inset shows a typical $F_{shear}(D)$ versus time plot for the highly-compressed ($D<D_0$) region of the plot, for PS−X(3.75×10^5) brushes compressed to surface separation D = 190 Å (corresponding to $D/2L=0.083$); sliding velocity 38 nm s^{-1}; the change in sign of F_{shear} at 38 and 76 s corresponds to a reversal of the sliding direction at these times.

ciated with this mutal intertanglement; but as noted earlier, in the regime of low friction $2L < D < D_0$ any changes in F_{shear} with v_s were below the resolution δF_{shear} of our measurements.

At the highest compressions sliding friction increases as these relaxations become sluggish. Partly this is because the effect of mutal intertanglement of the brushes increases at higher concentrations; but mainly, we believe, it is due to divergence of the relaxation times as the polystyrene in the gap approaches a glassy phase. (Polymer films only a few nanometres thick can have a glass transition temperature similar to that in the bulk[17].) The concentration c of polymer in a brush layer may be evaluated from the brush height L and its surface density (Table 1). For an uncompressed PS−X(1.4×10^5) brush (say), $c \approx 4.5\%$ w/v and varies inversely with D at $D < 2L$. For a compression ratio $(D/2L) = 0.1$, $c \approx 45\%$. The viscosity $\eta(c)$ of bulk polystyrene solutions at such high concentrations is high, and varies extremely rapidly with c. Typically, an increase in concentration from 45% to 55% in a solution of polystyrene, similar in size to the PS−X(1.4×10^5) chains, increases $\eta(c)$ by nearly an order of magnitude[18,19]. For PS−X(1.4×10^5) brushes, such an increase in c requires only a small change in $(D/2L)$: 0.1 to 0.08. Similar considerations apply to the other brushes. Although the shear mechanism of chains in a brush and in bulk polystyrene solutions differs[15,16], it is likely that the relative increase in their viscosity—and thus in viscous dissipation—with c is comparable[19]. This is consistent with the very sharp rise in the shear force as D decreases at $D < D_0$. Brushes consisting of polymers with low glass transition temperatures should thus be better lubricants at high compressions.

The precise frictional mechanism is very different to the classic interfacial sliding picture of Tabor and Bowden[4,20] and remains to be elucidated. Our observations reveal that a very fluid layer can reside at the interface between two solvated polymer brushes even under appreciable mutual compression, and can profoundly reduce the forces required for interfacial sliding of the surfaces bearing them. These results offer insight into relaxation processes in confined polymer layers and into tribological processes involving macromolecular surface phases. They also shed light on the origin of the very low friction in biological joints[21,22], where polymer-covered surfaces frequently rub against each other. Together with the self-assembling, robust and self-healing nature of polymer brushes, our results have clear implications for new lubrication strategies. □

Received 24 February; accepted 7 July 1994.

1. Tabor, D. *Friction* (Doubleday, New York, 1973).
2. Dowson, D. *History of Tribology* (Longmans, London, 1979).
3. Singer, I. L. & Pollock, H. M. (eds) *Fundamentals of Friction: Microscopic and Macroscopic Processes* (Kluwer, Dordrecht, 1992).
4. Tabor, D. in *Microscopic aspects of adhesion and lubrication* (ed. Georges, J. M.) 651–682 (Elsevier, New York, 1982).
5. Klein, J., Perahia, D. & Warburg, S. *Nature* **352,** 143–145 (1991).
6. Klein, J. *Pure appl. Chem.* **64,** 1577–1584 (1992).
7. Christenson, H. K. *J. chem. Phys.* **78,** 6906–6913 (1983).
8. Gee, M. L., McGuiggan, P. M., Israelachvili, J. N. & Homola, A. M. *J. chem. Phys.* **93,** 1895–1906 (1990).
9. Taunton, H. J., Toprakcioglu, C., Fetters, L. J. & Klein, J. Macromolecules **23,** 571–580 (1990).
10. Alexander, S. *J. Phys. Paris* **38,** 983–989 (1977).
11. de Gennes, P. G. *Adv. Colloid Interface Sci.* **27,** 189–207 (1987).
12. Halperin, A., Tirrell, M. & Lodge, T. *Adv. Polymer Sci.* **100,** 31–96 (1991).
13. Flory, P. J. *Principles of Polymer Chemistry* (Cornell Univ. Press, Ithaca, 1953).
14. de Gennes, P. G. in *Scaling Concepts in Polymer Physics* (Cornell Univ. Press, Ithaca, 1975).
15. Witten, T., Leibler, L. & Pincus, P. *Macromolecules* **23,** 824–830 (1990).
16. Joanny, J.-F. *Langmuir* **8,** 989–995 (1992).
17. Jackson, C. L. & McKenna, G. B. *J. non-cryst. Solids* 131–133, 221–224 (1991).
18. Graessley, W. W., Hazleton, R. L. & Lindeman, L. R. *Trans. Soc. Rheology* **11,** 267–285 (1967).
19. Utracki, L. A. & Roovers, J. E. L. *Macromolecules* **6,** 366–372 (1973).
20. Bowden, F. P. & Tabor, D. *The Friction and Lubrication of Solids* (Clarendon, Oxford, 1950).
21. McCutchen, C. W. *Nature* **184,** 1284–1286 (1959).
22. Maroudas, A. in *Lubrication and Wear in Joints* (ed. Wright, V.) Ch. 14. (Sector, London, 1969).

ACKNOWLEDGEMENTS. We thank M. Tirrell, A. Maroudas, P. Pincus, S. Granick and particularly D. Tabor for discussions. Support from the Israeli Ministry of Science, the Juelich Forschungszentrum, the Minerva Foundation, the Levin Fund and the Israeli National Science Foundation are acknowledged with thanks. J.F. is the Herman Mark Chair of Polymer Physics at the Weizmann Institute.

Polymeric fullerene chains in RbC_{60} and KC_{60}

Peter W. Stephens*, G. Bortel†, G. Faigel†, M. Tegze†, A. Jánossy†‡, S. Pekker†, G. Oszlanyi†§ & L. Forró§

* Department of Physics, State University of New York, Stony Brook, New York 11794, USA
† Research Institute for Solid State Physics, H-1525 Budapest, Hungary
‡ Technical University Budapest, Institute of Physics, H-1521 Budapest, Hungary
§ Laboratorie de Physique des Solides Semicrystallins, IGA, Department de Physique, Ecole Polytechnique Federal de Lausanne, 1015-Lausanne, Switzerland

NEARLY all of the molecular crystals containing C_{60} formed at ambient pressure[1,2] have inter-fullerene separations of the order of 10 Å—the expected distance based on the molecular van der Waals radii. The sole exceptions are the room-temperature phases of AC_{60} (where A denotes K, Rb or Cs), which are formed by reversible solid-state transformation from high-temperature (>150 °C) phases[3]. These phases have lattice parameters about 9% shorter in one direction, and in addition RbC_{60} has magnetic properties suggestive of a one-dimensional metal[4]. We suggested in ref. 4 that this short distance may be due to covalent bonding between neighbouring C_{60} molecules. Here we provide direct evidence for such bonding from powder X-ray diffraction studies of RbC_{60} and KC_{60}. The linkage is through a [2 + 2] cycloaddition, which has been hypothesized to take place during photopolymerization of solid C_{60} (ref. 5), and which has also been proposed[6] for RbC_{60}. Such inter-fullerene linkages are calculated[7,8] to be the preferred mode of dimerization of C_{60}. The AC_{60} phases thus provide an example of a thermal phase transition driven by the reversible formation and breaking of covalent bonds.

TABLE 1 Results of fits to various structural models for RbC_{60} and KC_{60}

Model		RbC_{60}			KC_{60}		
No.	Details	p	R_{WP}	F vs F_{95}	p	R_{WP}	F vs F_{95}
1.	Undistorted C_{60}, aligned with axes	13	13.7		22	12.3	
2.	Undistorted C_{60}, rotated ±45° about 9.11 Å direction	14	9.17	$75 \gg 4.0$	23	9.95	$25 \gg 4.0$
3.	Atoms C1 at inter-fullerene contact move in *a* direction.	15	6.19	$72 \gg 4.0$	24	7.43	$36 \gg 4.0$
4.	Atoms C1 move in molecular mirror plane	16	5.20	$24.6 \gg 4.0$	25	6.41	$15 \gg 4.0$
5.	Atoms C2 and C3 allowed to move, and overall C_{60} radius	20	4.85	$8.2 > 2.5$	29	5.78	$2.4 < 2.6$
6.	Same as 5, in *Immm*, with 50% C occupancy	20	4.93		29	6.19	

The fits shown here employ Rietveld fits to X-ray powder diffraction data[17]. p is the number of parameters adjusted in the fit, R_{WP} is the weighted profile crystallographic R factor, the F ratio is defined in the text, and F_{95} is the F ratio which would indicate a 95% ($\pm 2\sigma$) confidence limit on the improvement of the fit. For all Rietveld fits, we varied several diffraction lineshape parameters, the lattice parameters, the carbon isotropic thermal parameter, and anisotropic thermal parameters and fractional occupancy of the cation. The extra parameters for each KC_{60} fit are the intensity, lattice parameters, and lineshape parameters of coexisting C_{60} and K_3C_{60}.